

Politecnico di Bari

Repository Istituzionale dei Prodotti della Ricerca del Politecnico di Bari

Combining ad hoc spectral indices based on LANDSAT-8 OLI/TIRS sensor data for the detection of plastic cover vineyard

This is a post print of the following article

Original Citation:
Combining ad hoc spectral indices based on LANDSAT-8 OLI/TIRS sensor data for the detection of plastic cover vineyard / Novelli, A., Tarantino, E.. - In: REMOTE SENSING LETTERS. - ISSN 2150-704X. - STAMPA. - 6:12(2015), pp. 933-941. [10.1080/2150704X.2015.1093186]

Availability:
This version is available at http://hdl.handle.net/11589/5557 since: 2022-06-01

Published version
DOI:10.1080/2150704X.2015.1093186

Publisher:

Terms of use:

(Article begins on next page)

17 November 2026

TRSL_A_1093186
C/e: PS C/e QA: NA
Remote Sensing Letters, 2015
Vol. 00, No. 00, 1–9, http://dx.doi.org/10.1080/2150704X.2015.1093186

Taylor & Francis
Taylor & Francis Group

Combining ad hoc spectral indices based on LANDSAT-8 OLI/TIRS sensor data for the detection of plastic cover vineyard

AQ2 Antonio Novelli* and Eufemia Tarantino

AQ1 *DICATECH – Politecnico di Bari, Bari, Italy*

(*Received 18 June 2015; accepted 31 August 2015*)

In this article, we are proposing a method using Landsat-8 Operational Land Imager and Thermal Infrared Sensor data for agricultural plastic cover detection. Four normalized difference indices were combined in the procedure described to achieve consistent results: the green Normalized Difference Vegetation Index and three ad hoc spectral indices purposely created for this study (rescaled brightness temperature, Plastic Surface Index and Normalized Difference Sandy Index). The sampling time related to the preliminary collection of spectral information on plastic surfaces was reduced using information gathered through the Quality Assessment and Cloud Quality bands. The overall accuracies observed were on average higher than 80%,and the low cost of the open data set used, lacking ancillary data, demonstrated the reliability of the proposed method, proving its suitability for environmental and agricultural monitoring over large areas.

PROOF ONLY

1. Introduction

The widespread of plastic covering in agricultural practices (Espi et al. 2006) raises a significant issue in terms of anthropic impact on the original landscape (Picuno, Tortora, and Capobianco 2011). Due to its strategic economic importance, it seems necessary for this agricultural practice to be adequately monitored in order to avoid its uncontrolled development and its related consequences in rural areas (Briassoulis et al. 2013). Scientific literature proved that using high spatial resolution aerial/satellite data is one of the most important approach in managing the rapid expansion of plasticulture (Koç-San 2014; Agüera, Aguilar, and Aguilar 2008; Arcidiacono et al. 2012). Agüera and Liu (2009) proposed the use of Maximum Likelihood Classifier (MLC) and object-based classification of IKONOS and QuickBird data to delineate greenhouse areas. Plastic-covered vineyards in rural areas were mapped by Tarantino and Figorito (2012) using object-based classifications on true colours aerial photographs. Koc-San (2013) compared MLC, random forest and support vector machine to extract plastic and glass greenhouses. An unsupervised classification was carried out by Tasdemir and Koc-San (2014) in greenhouses detection. GeoEye-1 and WorldView2 stereo imagery were compared by Aguilar et al. (2014) in order to evaluate the enhancement in the extraction of greenhouses obtained from the combined use of spectral information, elevation data, band indexes and texture analysis.

Plastic cover detection is an active topic also in processing medium-resolution sensor data. Picuno, Tortora, and Capobianco (2011) performed a parallelepiped classification

*Corresponding author. Email: antonio.novelli@poliba.it

© 2015 Taylor & Francis

and GIS analysis on Landsat TM data to evaluate the impact of agricultural plastic covering. Plastic-mulched areas were studied by Lu, Di, and Ye (2014) using a decision-tree classifier on Landsat TM data. Lu, Hang, and Di (2015) showed a threshold model to extract plastic-mulched land covers from MODIS data.

Satellite thermal infrared (TIR) data are commonly processed for retrieving land surface temperature (LST) (Bai et al. 2015) and sea surface temperature (Tarantino 2012). Generally in-situ thermal data are necessary to study and assess growing conditions, air flow and evapotranspiration within greenhouses and to define experiment conditions (Villarreal-Guerrero et al. 2012). Yet, TIR sensor data can also be used as ancillary information to better discriminate surfaces with similar spectral response, hardly ever recognizable when applying the most consolidated methods (Crocetto and Tarantino 2009). Following their previous research experience, Novelli and Tarantino (2015) proposed a normalized difference index to test the contribution of Thermal Infrared Sensor (TIRS) data for fast plastic cover detection by working under simplified conditions (i.e. all non-agricultural pixels were excluded with a mask).

This article proposes a method for monitoring the spread of plastic covering in rural areas using multi-temporal free Landsat-8 Operational Land Imager (OLI) and TIRS sensor data, based on the implementation of four normalized indices: the Normalized Difference Vegetation Index (NDVI) green index and three spectral indices purposely created for this study (rescaled brightness temperature, Plastic Surface Index and Normalized Difference Sandy Index). The preliminary Quality Assessment (QA) band analysis was found to be crucial in the sampling process of plastic covered surfaces.

2. Data and study area

In this study, four Landsat-8 scenes along the same path-row were processed (Table 1), considering the summer period in which the plastic cover density is the highest. Landsat-8 OLI and TIRS sensors data can be freely selected through the USGS EROS web site (http://glovis.usgs.gov/) and are nominally processed as Level 1 terrain corrected (Roy et al. 2014).

The study area falls under the Province of Taranto in the Apulia Region (Southern Italy) (Figure 1). The western and the eastern bounds are, respectively, within the municipalities of Ginosa and Palagiano, close to the Ionian Sea. The climate is semi-arid and typically Mediterranean. Particularly, vineyards grow using the traditional grape cultivation system characterized by a supporting structure generally covered with plastic nets or sheets.

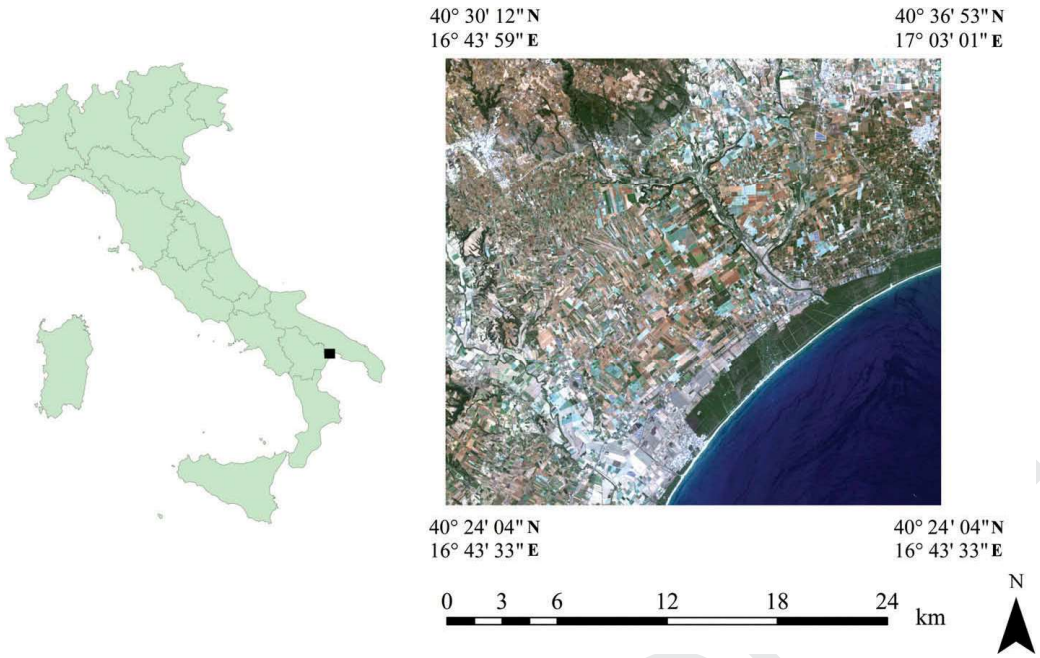
3. Method

The proposed methodology was aimed at the fast extraction of agricultural plastic covered area under the hypothesis of lacking updated ancillary data (i.e. technical cartography) and

Table 1. Scenes used in this study.

Acquisition date	Scene ID	Subset	Average cloud cover (%)
8 September 2013	LC81880322013251LGN00	*A*	1.56
7 August 2013	LC81880322013219LGN00	*B*	0.46
24 September 2014	LC81880322013267LGN00	*C*	0.31
10 August 2014	LC81880322014222LGN00	*D*	0.64

PROOF ONLY



COLOUR FIGURE

Figure 1. The study area (RGB visualization) within the Province of Taranto in the Apulia Region (Southern Italy).

using only free imagery. The method included the following steps: OLI and TIRS data pre-processing, definition of normalized difference indices and surface extraction.

3.1. *Data pre-processing and sampling of plastic cover reference areas*

The OLI digital numbers of the four Landsat images were linearly converted to sensor Top of Atmosphere (TOA) reflectance and then corrected for the sun angle using gains, offsets and local sun elevation values stored in each scene metadata. No atmospheric correction was performed in order to test the efficiency of the proposed index apart from local atmospheric noise and to reduce computation time.

QA bands were also used with the aim to mask cloud covered or corrupted pixels of each subset, testing their possible contribution to the method. Each pixel in the QA band contains a decimal value that represents a bit-packed combination of surface, atmosphere and sensor conditions that can affect the overall usefulness of a given pixel. Nine different bands can be extracted for every QA band. Three of them are1-bit bands (fill, dropped frame, terrain occlusion) and six of them are 2-bit bands (water, cloud shadow, vegetation, snow ice, cirrus, cloud). QA band data were unpacked though the L-LDOPE Toolbelt, a no-cost tool available from the USGS Landsat-8 website (Roy et al. 2002). In this case, all the nine bands were extracted at the default confidence level (34–66%) and only the Water and Cloud QA bands revealed a largely occurrence in the study area. The Water QA band showed a positive occurrence for luxuriant vegetation as well as for water. The Cloud QA band showed a positive occurrence not only for clouds but also for plastic covers and some urban areas. This last occurrence was found negligible if compared to the analogous agricultural plastic-covered areas. The Cloud QA band misclassified pixels were exploited in the next phase of the procedure for time saving in the sampling process of ground reference plastic-covered areas. For this purpose, the pixels common in each scene were

collected by intersecting the four Cloud QA bands. The results of this computation highlighted an evident connection between the Cloud quality band and agricultural plastic-covered surfaces. As a consequence, a slight manual input was required in order to sample more than 5000 pixels as ground reference for plastic-covered areas.

Lastly, thermal data were preprocessed. Recent literature has evidenced some calibration problems in Landsat-8 TIRS radiometric calibration for LST retrieval (Montanaro et al. 2014). This drawback was not considered in this study case because the first of the two TIRS channels was only used as ancillary information. Particularly, for each scene TIRS data were converted to at-satellite brightness temperature using the constants and the logarithmic formula provided by the USGS EROS web site.

3.2. *Defining ad hoc normalized difference indices to extract plastic cover surfaces*

Four normalized difference indices were used for the extraction of agricultural plastic-covered areas and they proved to be easy to compute, providing accurate results. Moreover, they performed better than a simple band ratio and, as dimensionless numbers, they were less sensitive to local conditions within the scene. The general approach for such index typology is to find out the strongest and weakest bands for the interested land cover type (Xu 2010). Their combination through a normalized difference can maximize the contrast between the interested cover type and others areas (referred as noise). The four indices were used simultaneously to reduce the commission between vegetation and bright plastic-covered surfaces.

The first index (1) was created to rescale the brightness temperature domain by standardizing its values range with the OLI-TOA reflectance values which were defined into a closed interval [0;1].

$$T_{\mathrm{bres}} = \frac{T_{\mathrm{b}} - T_{\mathrm{bmin}}}{T_{\mathrm{bmax}} - T_{\mathrm{bmin}}} \tag{1}$$

where T_{bres} is the rescaled brightness temperature; T_{b}, T_{bmin} and T_{bmax} are, respectively, the brightness temperature, the maximum and the minimum brightness temperature values for each subset.

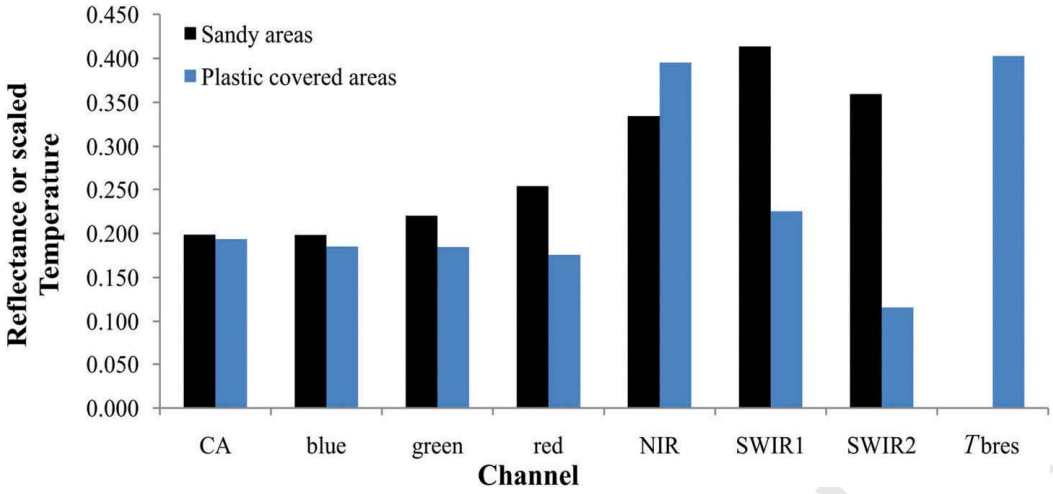
To better discriminate plastic covers from vegetation, the green Normalized Difference Vegetation Index ($\mathrm{NDVI}_{\mathrm{green}}$) (2) was implemented due to its better sensitivity to chlorophyll pigment (Gitelson, Kaufman, and Merzlyak 1996; Rivero et al. 2009):

$$\mathrm{NDVI}_{\mathrm{green}} = \frac{\rho_{\mathrm{NIR}} - \rho_{\mathrm{green}}}{\rho_{\mathrm{NIR}} + \rho_{\mathrm{green}}} \tag{2}$$

where ρ_{NIR} and ρ_{green} are, respectively, the reflectance in the green and near infrared (NIR) spectral bands.

The last two indices were created by using the information gained through sampled pixels. The aim was to emphasize agricultural plastic covered surfaces and to highlight bright surfaces to be removed. A small group of pixels corresponding to sandy shore areas was manually collected as representative of high reflectance surfaces in the visible domain. Figure 2 shows the mean values of the sampled pixels related to plastic covered areas and sandy areas for each considered channel.

PROOF ONLY



COLOUR FIGURE

Figure 2. Mean values of sampled pixels over the four subsets. The thermal channel was used only for plastic-covered areas to enhance their detection.

For plastic-covered areas, the strongest responses were in the NIR and in the T_{bres} channels while the weakest responses were in the red channel and in the second shortwave NIR band (SWIR2). High reflectance in the NIR band was not considered due to the high vegetation response in that channel. Based on the above assumptions, the most feasible channels for plastic-covered areas were the T_{bres}, the red and SWIR2 channels. The SWIR2 channel was combined with the T_{bres} channel through an arithmetic mean due to better results produced by this configuration. The formulation of Plastic Surface Index (PSI) (Novelli and Tarantino 2015) is shown in Equation (3).

$$PSI = \frac{\rho_{red} - \left(\frac{T_{bres}+\rho_{SWIR2}}{2}\right)}{\rho_{red} + \left(\frac{T_{bres}+\rho_{SWIR2}}{2}\right)} \quad (3)$$

The last created index involved the strongest response of the SWIR1band and the weakest response of the Costal Areosol (CA)band. It was named Normalized Difference Sandy Index (NDSI) and it assumed the following formulation (Equation (4)):

$$NDSI = \frac{\rho_{SWIR1} - \rho_{CA}}{\rho_{SWIR1} + \rho_{CA}} \quad (4)$$

3.3. *Using accuracy for extracting plastic-covered areas*

The above-mentioned indices were used to generate four binary raster masks (Equation (5)). Plastic cover extraction was carried out by simply intersecting the masks (Equation (6)).

$$Mask_i = index_i < (or >) threshold \quad (5)$$

$$\text{Plastic Surfaces} = \bigcap_{i=1}^{4} \text{Mask}_i \quad (6)$$

PROOF ONLY

Table 2. Ranges of the investigated thresholds for each proposed index.

Index	T_{bres}	$NDVI_{green}$	PSI	NDSA
Inequality	Greater than	Less than	Greater than	Less than
Value range	[0.00;0.29]	[−0.40;-0.11]	[−0.40;-0.11]	[0.00;0.29]

where for each *i*-th normalized difference index (i.e. T_{bres}, $NDVI_{green}$, PSI, NDSI) the threshold is a value extracted from an investigated range of the *i*-th index values (see Table 2). The final extraction was considered as a binary classification into the 'plastic surfaces' class and the general 'other' class. Lastly, the performance of the method was evaluated through the overall accuracy (OA) computed through the error matrix. An effective unbiased error matrix could be achieved only if each pixel of a given scene has a definite ground reference but this case is extremely time expensive. In many works, a stratified sampling strategy was implemented while the unbiased summary statistics would require the computation of a population matrix (Pontius Jr and Millones 2011). In this study case, the error matrix was evaluated using a similar number of ground reference for the two classes (more than 5000 pixels per class). Particularly, references related to the 'other' class were chosen within the most problematic areas: mixed classes and urban areas near the sampled pixels retrieved through the Cloud QA bands. The thresholds of each index were then evaluated by means of an IDL procedure (ENVI 2008) seeking the combinations of the four thresholds which maximize the OA: the appropriate thresholds were searched within ranges of the index values associated to the sampled pixels of plastic covered areas. Table 2 shows the range of values investigated (30 intervals of size 0.01) for each index and the inequality typology between the *i*-th index and its associated threshold.

For each combination of indices, Equations (5) and (6) were applied, the related error matrix was evaluated and then the OA of the extraction computed. The values of the index thresholds corresponding to the highest OA achieved for each subset where inserted in Equation (5) carrying out the final extraction (Equation (6)).

4. Results

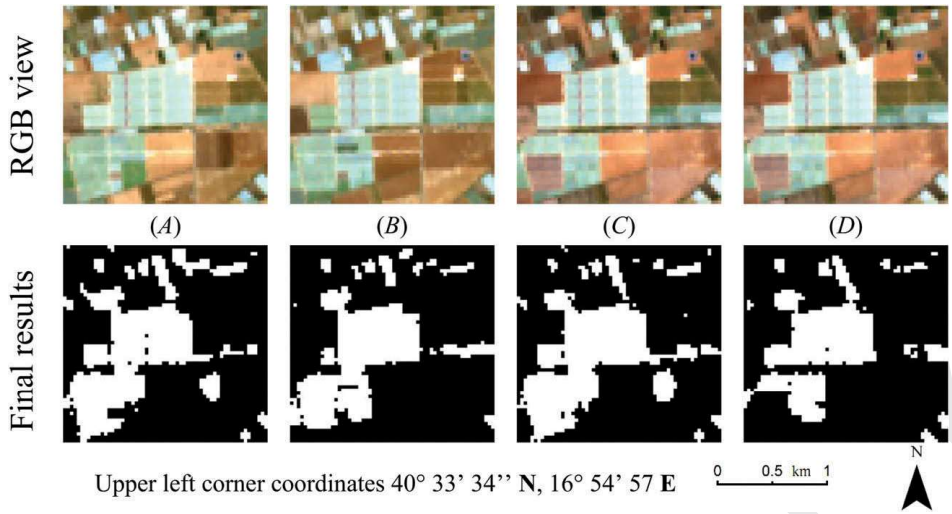
The best results representative of the extraction performed for each scene are shown in Table 3.

Figures 3 and 4 show the capability of the performed method and examples of commission error, respectively. The method performs well for plastic sheet placed above plastic net, generally bright in a true colour visualization. Despite plastic nets can

Table 3. Values of the index thresholds corresponding to the highest OA achieved for each subset.

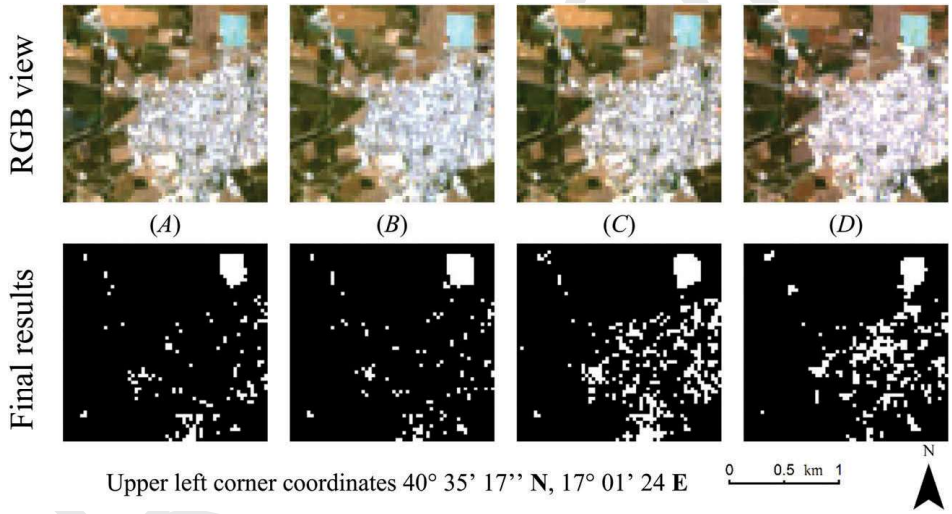
Subset	T_{bres}	$NDVI_{green}$	PSI	NDSA	OA (%)
A	0.25	−0.21	−0.38	0.27	86
B	0.29	−0.21	−0.39	0.27	89
C	0.12	−0.18	−0.35	0.29	84
D	0.25	−0.11	−0.40	0.28	82

PROOF ONLY



COLOUR FIGURE

Figure 3. Results for a small sample area related to the *A, B, C, D* subsets visualized in RGB to enhance the presence of plastic covers and in white to show the final detected areas.



COLOUR FIGURE

Figure 4. Results for a small urban/rural sample area related to the *A, B, C, D* subsets visualized in RGB to enhance the presence of plastic covers and in white to show the final detected objects mixed with false positive areas.

be very difficult to detect through Landsat data due to their high transmittance, the proposed method also extracts plastic nets with dense trammel.

The method revealed some commission errors within urban areas (Figure 4). A manually drawn binary mask was used for a further countercheck of the maximum OA found (89%). The binary mask covered built-up areas, and by intersecting the extracted pixels with the mask, it was possible to isolate and count commission pixels. The ratio between the number of commission pixels and the number of all extracted pixels showed that 11% of extracted pixels are part of built-up areas: the OA evidenced a good estimate of the real accuracy.

5. Conclusion

In this work, Landsat-8 OLI and TIRS sensor data were conjunctly used for agricultural plastic cover detection, testing four normalized difference indices. The procedure benefitted from the use of information gathered through the QA and Cloud Quality bands. Particularly, the use of Cloud Quality bands reduced sampling time and improved the collection of spectral information related to plastic surfaces. The overall accuracies observed were on average higher than 80%, and the low cost of the used open data set, lacking ancillary data, demonstrated the reliability of the proposed method, proving its suitability for environmental and agricultural monitoring over large areas.

Disclosure statement

AQ3 No potential conflict of interest was reported by the authors.

ORCID

Antonio Novelli http://orcid.org/0000-0002-5671-9220
Eufemia Tarantino http://orcid.org/0000-0002-2468-0771

References

Agüera, F., F. J. Aguilar, and M. A. Aguilar. 2008. "Using Texture Analysis to Improve Per-Pixel Classification of Very High Resolution Images for Mapping Plastic Greenhouses." *ISPRS Journal of Photogrammetry and Remote Sensing* 63 (6): 635–646. doi:10.1016/j.
AQ4 isprsjprs.2008.03.003.

Agüera, F., and J. G. Liu. 2009. "Automatic Greenhouse Delineation from Quickbird and Ikonos Satellite Images." *Computers and Electronics in Agriculture* 66 (2): 191–200. doi:10.1016/j.compag.2009.02.001.

Aguilar, M. A., F. Bianconi, F. J. Aguilar, and I. Fernández. 2014. "Object-Based Greenhouse Classification from Geoeye-1 and Worldview-2 Stereo Imagery." *Remote Sensing* 6 (5): 3554–3582. doi:10.3390/rs6053554.

Arcidiacono, C., S. M. C. Porto, and G. Cascone. 2012. "Accuracy of Crop-Shelter Thematic Maps: A Case Study of Maps Obtained by Spectral and Textural Classification of High-Resolution Satellite Images." *Journal Food Agricultural Environment* 10 (10711074): 18.

Bai, Y., M. S. Wong, W.-Z. Shi, L.-X. Wu, and K. Qin. 2015. "Advancing of Land Surface Temperature Retrieval Using Extreme Learning Machine and Spatio-Temporal Adaptive Data Fusion Algorithm." *Remote Sensing* 7 (4): 4424–4441. doi:10.3390/rs70404424.

Briassoulis, D., E. Babou, M. Hiskakis, G. Scarascia-Mugnozza, P. Picuno, D. Guarde, and C. Dejean. 2013. "Review, Mapping and Analysis of the Agricultural Plastic Waste Generation and Consolidation in Europe." *Waste Management & Research* 31 (12): 1262–1278. doi:10.1177/0734242X13507968.

Crocetto, N., and E. Tarantino. 2009. "A Class-Oriented Strategy for Features Extraction from Multidate ASTER Imagery." *Remote Sensing* 1 (4): 1171–1189. doi:10.3390/rs1041171.

ENVI User's Guide. 2008. "ENVI On-Line Software User's Manual." ITT Visual Information
AQ5 Solutions.

Espi, E., A. Salmeron, A. Fontecha, Y. García, and A. I. Real. 2006. "Plastic Films for Agricultural Applications." *Journal of Plastic Film and Sheeting* 22 (2): 85–102. doi:10.1177/8756087906064220.

Gitelson, A. A., Y. J. Kaufman, and M. N. Merzlyak. 1996. "Use of a Green Channel in Remote Sensing of Global Vegetation from EOS-MODIS." *Remote Sensing of Environment* 58 (3): 289–298. doi:10.1016/S0034-4257(96)00072-7.

Koc-San, D. 2013. "Evaluation of Different Classification Techniques for the Detection of Glass and Plastic Greenhouses from Worldview-2 Satellite Imagery." *Journal of Applied Remote Sensing* 7 (1): 073553. doi:10.1117/1.JRS.7.073553.

PROOF ONLY

Koç-San, D. 2014. "Thematic Mapping of Urban Areas from Worldview-2 Satellite Imagery Using Machine Learning Algorithms." *Journal of Geodesy and Geoinformation* 2 (1).

Lu, L., L. Di, and Y. Ye. 2014. "A Decision-Tree Classifier for Extracting Transparent Plastic-Mulched Landcover from Landsat-5 TM Images." *IEEE Journal of Selected Topics in Applied Earth Observations and Remote Sensing* 7 (11): 4548–4558. doi:10.1109/JSTARS.2014.2327226.

Lu, L., D. Hang, and L. Di. 2015. "Threshold Model for Detecting Transparent Plastic-Mulched Landcover Using Moderate-Resolution Imaging Spectroradiometer Time Series Data: A Case Study in Southern Xinjiang, China." *Journal of Applied Remote Sensing* 9 (1): 097094. doi:10.1117/1.JRS.9.097094.

Montanaro, M., A. Gerace, A. Lunsford, and D. Reuter. 2014. "Stray Light Artifacts in Imagery from the Landsat 8 Thermal Infrared Sensor." *Remote Sensing* 6 (11): 10435–10456. doi:10.3390/rs61110435.

Novelli, A., and E. Tarantino. 2015. "The Contribution of Landsat 8 TIRS Sensor Data to the Identification of Plastic Covered Vineyards." *Proceeding of SPIE 9535, Third International Conference on Remote Sensing and Geoinformation of the Environment (RSCy2015), 95351E.*

Picuno, P., A. Tortora, and R. L. Capobianco. 2011. "Analysis of Plasticulture Landscapes in Southern Italy through Remote Sensing and Solid Modelling Techniques." *Landscape and Urban Planning* 100 (1–2): 45–56. doi:10.1016/j.landurbplan.2010.11.008.

Pontius Jr, R. G., and M. Millones. 2011. "Death to Kappa: Birth of Quantity Disagreement and Allocation Disagreement for Accuracy Assessment." *International Journal of Remote Sensing* 32 (15): 4407–4429. doi:10.1080/01431161.2011.552923.

Rivero, R. G., S. Grunwald, M. W. Binford, and T. Z. Osborne. 2009. "Integrating Spectral Indices into Prediction Models of Soil Phosphorus in a Subtropical Wetland." *Remote Sensing of Environment* 113 (11): 2389–2402. doi:10.1016/j.rse.2009.07.015.

Roy, D. P., J. S. Borak, S. Devadiga, R. E. Wolfe, M. Zheng, and J. Descloitres. 2002. "The MODIS Land Product Quality Assessment Approach." *Remote Sensing of Environment* 83 (1–2): 62–76. doi:10.1016/S0034-4257(02)00087-1.

Roy, D. P., M. A. Wulder, T. R. Loveland, W. Ce, R. G. Allen, M. C. Anderson, D. Helder, J. R. Irons, D. M. Johnson, and R. Kennedy. 2014. "Landsat-8: Science and Product Vision for Terrestrial Global Change Research." *Remote Sensing of Environment* 145: 154–172. doi:10.1016/j.rse.2014.02.001.

Tarantino, E. 2012. "Monitoring Spatial and Temporal Distribution of Sea Surface Temperature with TIR Sensor Data." *Italian Journal of Remote Sensing* 44 (1): 97–107. doi:10.5721/ItJRS.

Tarantino, E., and B. Figorito. 2012. "Mapping Rural Areas with Widespread Plastic Covered Vineyards Using True Color Aerial Data." *Remote Sensing* 4 (12): 1913–1928. doi:10.3390/rs4071913.

Tasdemir, K., and D. Koc-San. 2014. "Unsupervised Extraction of Greenhouses Using Worldview-2 Images." Paper presented at the International Geoscience and Remote Sensing Symposium (IGARSS).

Villarreal-Guerrero, F., M. Kacira, E. Fitz-Rodríguez, C. Kubota, G. A. Giacomelli, R. Linker, and A. Arbel. 2012. "Comparison of Three Evapotranspiration Models for a Greenhouse Cooling Strategy with Natural Ventilation and Variable High Pressure Fogging." *Scientia Horticulturae* 134: 210–221. doi:10.1016/j.scienta.2011.10.016.

Xu, H. 2010. "Analysis of Impervious Surface and Its Impact on Urban Heat Environment Using the Normalized Difference Impervious Surface Index (NDISI)." *Photogrammetric Engineering & Remote Sensing* 76 (5): 557–565. doi:10.14358/PERS.76.5.557.

PROOF ONLY